

THEORY AND INTERNAL STRUCTURE OF ADER-DG METHOD FOR ORDINARY DIFFERENTIAL EQUATIONS*

IVAN S. POPOV†

Abstract. Investigation of the approximation properties, convergence, and stability of the ADER-DG method for solving an ODE system is carried out. The ADER-DG method generates a new implicit RK method, which is similar in its properties to the original ADER-DG method. The ADER-DG method has an approximation order $2N + 1$ when using polynomials of degree N for the numerical solution at grid nodes, and demonstrates superconvergence. The local solution obtained by the local DG predictor has an approximation order $N + 1$ and has a subgrid resolution. The ADER-DG method is A - and AN -stable, L -stable, B - and BN -stable, and algebraically stable. Applications of the ADER-DG method demonstrated compliance with the expected theoretical results.

Key words. Discontinuous Galerkin method, ADER-DG method, Local DG predictor, Implicit Runge-Kutta methods, Superconvergence, Convergence and approximation analysis, Stability analysis, First-order ODE systems

MSC codes. 65L05, 65L60, 65L20, 65L06

1. Introduction. In this paper, a study of the approximation properties, convergence and stability of arbitrary high order ADER (“Arbitrary-higher-order-DErivative”) discontinuous Galerkin (DG) method with local DG predictor for solving the initial value problem (IVP) for a system of ordinary differential equations (ODE) is carried out. The IVP for ODE system is chosen in the following classical form:

$$(1.1) \quad \frac{d\mathbf{u}}{dt} = \mathbf{F}(\mathbf{u}, t), \quad t \in \Omega = \{t \mid t \in [t_0, t_f]\}, \quad \mathbf{u}(t_0) = \mathbf{u}_0,$$

where $\mathbf{u} : \Omega \rightarrow \mathcal{R}^D$ is a desired function, $\mathbf{F} : \mathcal{R}^D \times \Omega \rightarrow \mathcal{R}^D$ is a right side function, which is given. The initial condition \mathbf{u}_0 on the desired function \mathbf{u} was chosen at the point t_0 . The classical ODE theory shows that in case $\mathbf{F} \in \mathcal{C}_1(\mathcal{R}^D \times \Omega)$ the solution of the problem exists and is unique. The ODE systems of the second and higher orders, uniquely solvable with respect to higher derivatives, can be represented in the form of the first-order ODE system (1.1).

ODE systems are used in a wide range of fields of science and technology. There are now many numerical methods for solving ODE systems [10, 26, 27]. In recent years, there has been increased scientific interest in studying DG methods and the associated superconvergence in solving ODE systems, see books [1, 41] and recent articles [2–7, 34]. DG methods were proposed in [37] for the numerical description of neutron transport. Delfour *et al* [18] proposed a DG method for solving ODE systems, then a rigorous theory on this basis was developed in [17]. Cockburn, Shu *et al.* in a series of works [11–15] created a rigorous mathematical basis for DG methods, which stimulated their further development and use for solving a wide class of problems.

The ADER-DG methods are DG methods based on the ADER paradigm proposed by Titarev and Toro in [38, 39] in the context of finite volume methods. The modern version of ADER involves the use of a local DG predictor, which was proposed by Dumbser *et al* [20, 29]. The use of ADER in DG methods has allowed obtaining unrivaled results in the numerical solution of systems of partial differential equations

*Submitted to the editors DATE.

†Department of Theoretical Physics, Dostoevsky Omsk State University, Omsk, Russia (diphosgen@mail.ru, popovis@omsu.ru).

(PDE) [9, 19, 21–25, 31, 33, 35, 40, 42, 43]. In Han Veiga *et al* [28] and Micalizzi *et al* [32] showed that the methods of the ADER family are significantly interconnected with numerical methods on the deferred correction (DeC) paradigm.

The use of the ADER-DG method for solving ODE systems was proposed in [34], based on the ideas in [19, 20]. ADER-DG has demonstrated high accuracy and stability in solving ODE systems, as well as systems of differential-algebraic equations [36]. However, these results are only empirical, based on qualitative considerations, numerical calculations, and solving a set of test problems.

Empirical results can not replace a rigorous theory, therefore, in this paper, a rigorous analytical study of the ADER-DG method as applied to ODE systems is carried out. The properties of approximation, convergence and stability of the ADER-DG method are investigated, and an implicit Runge-Kutta (RK) method, which is generated by the ADER-DG method and is equivalent to it, is found. The study is carried out for an arbitrary value of the degree of polynomials N .

2. Formulation of ADER-DG method. A description of the ADER-DG method for solving problem (1.1) was presented in [34, 36], therefore the description will be limited to what is necessary for this paper.

The numerical solution is found on a one-dimensional grid that discretizes the domain of definition Ω by a finite set $\{\Omega_n\}$ of non-overlapping discretization domains $\Omega_n = \{t \mid t \in [t_n, t_{n+1}]\}$, where t_n is the grid nodes, $\Delta t_n = t_{n+1} - t_n$ is the discretization step, and the discretization domains Ω_n themselves are called the space between the nodes. The numerical method is completely single-step, therefore the formula apparatus of the method itself is formulated only for one discretization domain Ω_n , and allows the use of a variable discretization step Δt_n . Due to the high accuracy of the ADER-DG method even on coarse grids [34, 36], it is possible to allow the use of a grid containing only one discretization domain $\Omega_1 = \Omega$.

The ADER-DG method is based on the integral form of the ODE system (1.1):

$$(2.1) \quad \mathbf{u}_{n+1} = \mathbf{u}_n + \int_{t_n}^{t_{n+1}} \mathbf{F}(\mathbf{u}(t), t) dt,$$

where \mathbf{u}_n and \mathbf{u}_{n+1} are the numerical solution at grid nodes t_n and t_{n+1} , respectively. In the integrand \mathbf{F} the function $\mathbf{u} = \mathbf{u}(t)$, explicitly dependent on t , is defined in the space Ω_n between the grid nodes t_n and t_{n+1} . To formulate the ADER-DG method and isolating its main structural components, the discretization domain Ω_n is mapped $t \mapsto \tau(t)$ onto the reference domain $\omega = \{\tau \mid \tau \in [0, 1]\}$:

$$(2.2) \quad t(\tau) = t_n + \tau \cdot \Delta t_n \in \Omega_n, \quad \tau(t) = \frac{t - t_n}{\Delta t_n} \in \omega,$$

where $\tau \in [0, 1]$ is the coordinate of the reference domain ω . The ADER-DG numerical method is based on the use of a local solution $\mathbf{q}_n : \omega \rightarrow \mathcal{R}^D$, which is defined in the space between the grid nodes Ω_n :

$$(2.3) \quad \mathbf{u} = \mathbf{u}(t(\tau)), t \in \Omega_n \mapsto \mathbf{q}_n = \mathbf{q}_n(\tau),$$

and is used to calculate the integral in (2.1). The local solution is also defined for the definition domain $\mathbf{u}_L : \Omega \rightarrow \mathcal{R}^D$ by a piecewise assembly of local solutions \mathbf{q}_n for each Ω_n :

$$(2.4) \quad \mathbf{u}_L(t) = \sum_n \chi_n(t) \cdot \mathbf{q}_n \left(\frac{t - t_n}{\Delta t_n} \right),$$

where $\chi_n : \Omega \rightarrow \{0, 1\}$ is the indicator function of the discretization domain $\Omega_n \subseteq \Omega$.

The original version of the ADER numerical methods [38,39] chose a local solution as expansion according to the Cauchy-Kovalevskaya procedure, which in the case of ODE systems is close to the families of high-order Taylor numerical methods [8,30]. The modern formulation of the ADER numerical methods [20,29] is based on the use of a DG predictor, in which the local solution is represented in the form of an expansion over a set $\{\varphi_p\}$ of basis functions $\varphi_p : \omega \rightarrow \mathcal{R}$ of the following form:

$$(2.5) \quad \mathbf{q}_n(\tau) = \sum_p \hat{\mathbf{q}}_{n,p} \varphi_p(\tau),$$

and is found as a solution to the weak form of the ODE system (1.1) in Ω_n :

$$(2.6) \quad \int_0^1 \varphi_p(\tau) \left[\frac{d\mathbf{q}_n(\tau)}{d\tau} - \Delta t_n \mathbf{F}(\mathbf{q}_n(\tau), t(\tau)) \right] = 0, \quad \mathbf{q}_n(0) = \mathbf{u}_n.$$

The basis functions are selected in the form of Lagrange interpolation polynomials $\{\varphi_p\}_{p=0}^N$ with nodal points at the roots of the shifted Legendre polynomials \tilde{P}_{N+1} :

$$(2.7) \quad \varphi_p(\tau) = \sum_{k=0}^N \varphi_{p,k} \tau^k = \prod_{k \neq p} \frac{\tau - \tau_k}{\tau_p - \tau_k}, \quad \varphi_p(\tau_q) = \delta_{pq},$$

where $\{\tau_k\}_{k=0}^N$ is an ascending order set of roots of the shifted Legendre polynomials \tilde{P}_{N+1} , $\{\varphi_{p,k}\}$ is a set of coefficients of the basis polynomials $\{\varphi_p\}$. The choice of the basis allowed to use the Gauss-Legendre (GL) quadrature formula:

$$(2.8) \quad \int_0^1 f(\tau) d\tau \approx \sum_{p=0}^N w_p f(\tau_p), \quad w_p = \int_0^1 \varphi_p^2(\tau) d\tau = \int_0^1 \varphi_p(\tau) d\tau > 0, \quad \sum_{p=0}^N w_p = 1,$$

where $\{w_p\}$ is the weights, to calculate integrals (2.1) and obtain point-wise evaluation

$$(2.9) \quad \mathbf{F}(\mathbf{q}_n(\tau), t(\tau)) = \sum_{p=0}^N \hat{\mathbf{F}}_{n,p} \varphi_p(\tau) \mapsto \sum_{p=0}^N \mathbf{F}(\hat{\mathbf{q}}_{n,p}, t(\tau_p)) \varphi_p(\tau).$$

Evaluating the expression (2.6) leads to a system of nonlinear algebraic equations:

$$(2.10) \quad \sum_{q=0}^N \left[\kappa_{pq} \hat{\mathbf{q}}_{n,q} - \Delta t_n \mu_{pq} \mathbf{F}(\hat{\mathbf{q}}_{n,q}, t(\tau_q)) \right] = \psi_p \mathbf{u}_n,$$

where the coefficients can be collected into matrices $\kappa = \|\kappa_{pq}\|$, $\mu = \|\mu_{pq}\|$ and calculated by the following expressions:

$$(2.11) \quad \begin{aligned} \kappa_{pq} &= \tilde{\psi}_p \tilde{\psi}_q - \int_0^1 \frac{d\varphi_p(\tau)}{d\tau} \varphi_q(\tau) d\tau = \psi_p \psi_q + \int_0^1 \varphi_p(\tau) \frac{d\varphi_q(\tau)}{d\tau} d\tau, \\ \mu_{pq} &= \int_0^1 \varphi_p(\tau) \varphi_q(\tau) d\tau \equiv w_p \delta_{pq}, \quad \psi_p = \varphi_p(0), \quad \tilde{\psi}_p = \varphi_p(1), \end{aligned}$$

where the last expression explicitly takes into account the orthogonality of the basis $\{\varphi_p\}$ and the expression for the weights w_p of the quadrature formula (2.8). Multiplication by κ^{-1} leads to the system of equations of the local DG predictor:

$$(2.12) \quad \hat{\mathbf{q}}_{n,p} = \mathbf{u}_n + \Delta t_n \sum_{q=0}^N a_{pq} \mathbf{F}(\hat{\mathbf{q}}_{n,q}, t(\tau_q)),$$

where a_{pq} is elements of the matrix $a = \kappa^{-1}\mu$, and Lemma 2.1 is taken into account.

LEMMA 2.1. *The parameters of the ADER-DG method satisfy the relations:*

$$(2.13) \quad \begin{aligned} \sum_{q=0}^N a_{pq} \psi_q &= w_p, & \sum_{q=0}^N [\kappa^{-1}]_{pq} \psi_q &= 1, & \psi_p &= \sum_{q=0}^N \kappa_{pq}, \\ \sum_{p=0}^N a_{pq} \tilde{\psi}_p &= w_q, & \sum_{p=0}^N [\kappa^{-1}]_{pq} \tilde{\psi}_p &= 1, & \tilde{\psi}_q &= \sum_{p=0}^N \kappa_{pq}, \\ \text{tr}(\kappa) &= \sum_{p=0}^N \kappa_{pp} = \frac{1}{2} \sum_{p=0}^N [\psi_p^2 + \tilde{\psi}_p^2] = \sum_{p=0}^N \psi_p^2 = \sum_{p=0}^N \tilde{\psi}_p^2. \end{aligned}$$

Proof. These relationships are proved by direct expansion of the expressions:

$$\begin{aligned} \sum_{q=0}^N a_{pq} \psi_q &= \sum_{q=0}^N [\kappa^{-1} \cdot \mu]_{pq} \psi_q = \sum_{q=0}^N \sum_{r=0}^N [\kappa^{-1}]_{pr} w_r \delta_{rq} \psi_q = w_p, \\ \sum_{p=0}^N a_{pq} \tilde{\psi}_p &= \sum_{p=0}^N [\kappa^{-1} \cdot \mu]_{pq} \tilde{\psi}_p = \sum_{p=0}^N \sum_{r=0}^N [\kappa^{-1}]_{pr} w_r \delta_{rq} \tilde{\psi}_p = w_q, \\ \sum_{q=0}^N a_{pq} \psi_q &= w_p \Leftrightarrow \sum_{q=0}^N [\kappa^{-1}]_{pq} \psi_q = 1 \Leftrightarrow \psi_p = \sum_{q=0}^N \kappa_{pq}, \\ \sum_{p=0}^N a_{pq} \tilde{\psi}_p &= w_q \Leftrightarrow \sum_{p=0}^N [\kappa^{-1}]_{pq} \tilde{\psi}_p = 1 \Leftrightarrow \tilde{\psi}_q = \sum_{p=0}^N \kappa_{pq}, \\ \sum_{q=0}^N \kappa_{pq} &= \left| \sum_{p=0}^N \varphi_p(\tau) \equiv 1 \right| = \psi_p \sum_{p=0}^N \psi_q + \int_0^1 \varphi_p(\tau) \frac{d}{d\tau} \left[\sum_{q=0}^N \varphi_q(\tau) \right] d\tau = \psi_p, \\ \sum_{p=0}^N \kappa_{pq} &= \tilde{\psi}_q \sum_{p=0}^N \tilde{\psi}_p - \int_0^1 \varphi_q(\tau) \frac{d}{d\tau} \left[\sum_{p=0}^N \varphi_p(\tau) \right] d\tau = \tilde{\psi}_p, \\ \text{tr}(\kappa) &= \sum_{p=0}^N \kappa_{pp} = \sum_{p=0}^N \left[\tilde{\psi}_p \tilde{\psi}_p - \int_0^1 \frac{d\varphi_p(\tau)}{d\tau} \varphi_p(\tau) d\tau \right] \\ &= \sum_{p=0}^N \left[\tilde{\psi}_p \tilde{\psi}_p - \frac{1}{2} (\tilde{\psi}_p \tilde{\psi}_p - \psi_p \psi_p) \right] = \frac{1}{2} \sum_{p=0}^N [\psi_p^2 + \tilde{\psi}_p^2] = \sum_{p=0}^N \psi_p^2 = \sum_{p=0}^N \tilde{\psi}_p^2, \end{aligned}$$

where in the last two identities the symmetry property $\tau_p = 1 - \tau_{N-p}$ of the zeros of shifted Legendre polynomials \tilde{P}_{N+1} was used, resulting in $\varphi_p(\tau) = \varphi_{N-p}(1 - \tau)$, in particular, $\tilde{\psi}_p = \psi_{N-p}$, so the sums are the same. \square

Remark 2.2. It can be noted that the second relation in (2.13) can be proved heuristically: in the case of $\mathbf{F} \equiv 0$, the solution \mathbf{q}_n to the problem (2.6) is a constant, but the initial condition $\mathbf{q}_n(0) = \mathbf{u}_n$ assumes $\mathbf{q}_n(\tau) \equiv \mathbf{u}_n$, from which the relation (2.13) to be proven directly. Otherwise $\mathbf{F} \not\equiv 0$, the values κ_{pq} and ψ_p do not depend on \mathbf{F} by construction, which reduces the proof to the case $\mathbf{F} \equiv 0$.

Remark 2.3. The relations presented in the Lemma 2.1 do not depend on the explicit choice of Legendre polynomials \tilde{P}_{N+1} and can also be used with other polynomials, such as the left and right Rado polynomials. However, the last transformation of the symmetrized sum into individual sums requires symmetry of the roots $\{\tau_p\}$.

Remark 2.4. These relations can be useful not only in proving theorems, but also in software development, especially in testing and formulating assertions, or simplifying expressions, such as making the factor around \mathbf{u}_n disappear in (2.12).

The resulting system of equations (2.12) is generally nonlinear and can be solved by Newton's or Picard's iteration methods, as well as other methods for solving systems of nonlinear algebraic equations. The existence and uniqueness of a solution to the system of equations (2.12), which in this case can be obtained by iteration, is guaranteed under the conditions presented in Remark 3.3.

The expression (2.1) of the solution \mathbf{u}_{n+1} at the grid node t_{n+1} as a result of using the quadrature formula (2.8) takes the form:

$$(2.14) \quad \mathbf{u}_{n+1} = \mathbf{u}_n + \Delta t_n \sum_{p=0}^N w_p \mathbf{F}(\hat{\mathbf{q}}_{n,p}, t(\tau_p)).$$

The expressions (2.12), (2.14) together constitute the ADER-DG method for solving the IVP for an ODE system (1.1).

The solution \mathbf{u}_{n+1} at the grid node t_{n+1} and the local solution $\mathbf{q}_n(1)$ coincide:

$$(2.15) \quad \mathbf{q}_n(1) = \sum_{p=0}^N \hat{\mathbf{q}}_{n,p} \tilde{\psi}_p = \mathbf{u}_n + \Delta t_n \sum_{q=0}^N \left[\sum_{p=0}^N a_{pq} \tilde{\psi}_p \right] \mathbf{F}(\hat{\mathbf{q}}_{n,q}, t(\tau_q)) \equiv \mathbf{u}_{n+1},$$

which is associated with a property of the parameters expressed by Lemma 2.1. It can not rigorously explain superconvergence of the solution of algebraic variables in [36].

3. ADER-DG method as Runge-Kutta method. The use of substitution

$$(3.1) \quad \hat{\mathbf{q}}_{n,p} = \mathbf{u}_n + \Delta t_n \sum_{q=0}^N a_{pq} \mathbf{k}_q,$$

known in the theory of Runge-Kutta (RK) methods [10, 16, 26, 27], in expressions (2.12), (2.14) allows to reformulate the ADER-DG method as the s -stage implicit RK method with $s = N + 1$:

$$(3.2) \quad \mathbf{k}_p = \mathbf{F} \left(\mathbf{u}_n + \Delta t_n \sum_{q=0}^N a_{pq} \mathbf{k}_q, t_n + \tau_p \cdot \Delta t_n \right), \quad \mathbf{u}_{n+1} = \mathbf{u}_n + \Delta t_n \sum_{p=0}^N w_p \mathbf{k}_p,$$

which in terms of weights $\{w_p\}$ and nodes $\{\tau_p\}$ corresponds to the implicit Gauss-Legendre (GL) method. However, the coefficients a_{pq} does not coincide with any RK method known (at least to the author). The set of coefficients $\{a_{pq}, w_p, \tau_p\}$ can be

exactly calculated in radicals for $N \leq 8$. In cases $N = 1, 2, 3$, the Butcher tables take the form:

$$(3.3) \quad \begin{array}{c|c|c|c|c} \frac{1}{2} - \frac{\sqrt{3}}{6} & \frac{1}{3} & -\frac{1-\sqrt{3}}{2} & \frac{1}{2} - \frac{\sqrt{15}}{10} & \frac{29}{180} & \frac{8}{45} - \frac{\sqrt{15}}{15} & \frac{29}{180} - \frac{\sqrt{15}}{30} \\ \frac{1}{2} + \frac{\sqrt{3}}{6} & \frac{1-\sqrt{3}}{2} & \frac{1}{3} & \frac{1}{2} + \frac{\sqrt{15}}{10} & \frac{1}{9} + \frac{\sqrt{15}}{24} & \frac{5}{18} & \frac{1}{9} - \frac{\sqrt{15}}{24} \\ \hline & \frac{1}{2} & \frac{1}{2} & & \frac{29}{180} + \frac{\sqrt{15}}{30} & \frac{8}{45} + \frac{\sqrt{15}}{15} & \frac{29}{180} \\ \hline & & & & \frac{5}{18} & \frac{4}{9} & \frac{5}{18} \end{array}$$

$$\begin{array}{c|c} \frac{1}{2} - \frac{\sqrt{525+70\sqrt{30}}}{70} & \left[\begin{array}{cccc} \frac{5\sqrt{30}}{72} + \frac{19}{24} & -\frac{43}{60} + \frac{17\sqrt{30}}{72} & -\frac{13}{40} & \frac{13}{28} - \frac{53\sqrt{30}}{630} \\ -\frac{43}{60} - \frac{17\sqrt{30}}{72} & -\frac{5\sqrt{30}}{72} + \frac{19}{24} & \frac{13}{28} + \frac{53\sqrt{30}}{630} & -\frac{13}{40} \\ \frac{1}{2} + \frac{\sqrt{525-70\sqrt{30}}}{70} & -\frac{27}{28} - \frac{47\sqrt{30}}{420} & -\frac{5\sqrt{30}}{72} + \frac{19}{24} & -\frac{43}{60} + \frac{17\sqrt{30}}{72} \\ \frac{1}{2} + \frac{\sqrt{525+70\sqrt{30}}}{70} & -\frac{27}{28} + \frac{47\sqrt{30}}{420} & \frac{47}{40} & -\frac{43}{60} - \frac{17\sqrt{30}}{72} \end{array} \right]^{-1} \\ \hline & \cdot \text{diag} \left(-\frac{\sqrt{30}}{72} + \frac{1}{4}, \frac{\sqrt{30}}{72} + \frac{1}{4}, \frac{\sqrt{30}}{72} + \frac{1}{4}, -\frac{\sqrt{30}}{72} + \frac{1}{4} \right) \\ \hline & \begin{array}{cccc} -\frac{\sqrt{30}}{72} + \frac{1}{4} & \frac{\sqrt{30}}{72} + \frac{1}{4} & \frac{\sqrt{30}}{72} + \frac{1}{4} & -\frac{\sqrt{30}}{72} + \frac{1}{4} \end{array} \end{array}$$

but already in the case $N = 3$, the expressions for the coefficients a_{pq} become large, therefore in the case of $N \geq 3$, it is more convenient to choose the coefficients a_{pq} numerically.

DEFINITION 3.1. *IRK-GL-ADER-DG method is the implicit RK method (3.2) based on ADER-DG method (2.12), (2.14) with nodal basis (2.7) in roots of Legendre polynomial P_{N+1} and using the GL quadrature formula (2.8).*

Remark 3.2. Calculation of Butcher tables $\{a_{pq}, w_p, \tau_p\}$ for left and right Rado polynomials showed that the results are completely consistent with the Butcher tables of Rado IA and IIA methods, respectively. Therefore, these results presented in the classical literature [10, 16, 27] are expected, and not considered in the this paper.

Remark 3.3. The ADER-DG method (2.12), (2.14) is equivalent to the implicit RK method, so to determine the existence and uniqueness of a solution $\{\hat{\mathbf{q}}_p\}$ one can use Theorem 7.2 in [26], according to which, if $\mathbf{F}(\mathbf{u}, t) \in \mathcal{C}_0(\Xi)$ satisfying the Lipschitz condition with constant $C > 0$ in neighborhood $\Xi \subseteq \mathcal{R}^D \times \Omega$ of the (\mathbf{u}_n, t_n) , and if

$$(3.4) \quad \Delta t_n \cdot C \max_p \sum_{q=0}^N |a_{pq}| < 1,$$

then the system of equations (2.12) has a unique solution $\{\hat{\mathbf{q}}_p\}$, which can be obtained by iteration. If also $\mathbf{F}(\mathbf{u}, t) \in \mathcal{C}_p(\Xi \times \Omega) \subset \mathcal{C}_0(\Xi \times \Omega)$, then $\{\hat{\mathbf{q}}_q(\Delta t_n) \in \mathcal{C}_p(\mathcal{R})\}_{q=0}^N$.

4. Superconvergence and orders. The determination of the approximation order of the ADER-DG method can now be carried out on the basis of the well-known theory of RK methods [10, 16, 26]. In this paper, simplifying conditions (see [16]) are used, which are formulated in terms of the parameters of the ADER-DG method:

$$(4.1) \quad \begin{aligned} B(L) : \sum_{q=0}^N w_q \tau_q^r &= \frac{1}{r+1}, \quad 0 \leq r < L, \\ C(L) : \sum_{q=0}^N a_{pq} \tau_q^r &= \frac{\tau_p^{r+1}}{r+1}, \quad 0 \leq p \leq N, \quad 0 \leq r < L, \\ D(L) : \sum_{q=0}^N w_q a_{qp} \tau_q^r &= \frac{w_p}{r+1} (1 - \tau_p^{r+1}), \quad 0 \leq p \leq N, \quad 0 \leq r < L. \end{aligned}$$

The nodes and weights of the quadrature formula (2.8) ensure (see also [16]) that condition $B(2N + 2)$ is satisfied, therefore, to determine the approximation order, it is necessary to study conditions $C(L)$ and $D(L)$.

The conditions (4.1) were verified numerically using module `mpmath` (with internal use of module `gmpy2`, based on the MPFR numerical library) of the `python` programming language, with an arithmetic precision constant `mpmath.mp.dps = 1000`. Numerical investigation of cases $N = 1, \dots, 75$ showed that conditions $C(N)$, $D(N)$ are satisfied with precision 10^{-978} – 10^{-1006} . However, conditions $C(N + 1)$, $D(N + 1)$, which are inherent in the classical GL method are not satisfied, but the deviations decrease with N , reaching 10^{-48} – 10^{-49} for $C(N + 1)$ and 10^{-50} – 10^{-52} for $D(N + 1)$ in case $N = 75$. Based on expected result, a rigorous proof is created, presented by Theorem 4.9. In the classical GL method, the proof is based on the property $a_{pq} = \int_0^{\tau_p} \varphi_q(\tau) d\tau$, however, in this case, it is obviously not satisfied.

LEMMA 4.1. *The local solution q_n (2.5) is the exact solution of the ODE*

$$(4.2) \quad \frac{du}{dt} = f(t), \quad f(t) \in \mathcal{P}_L(\mathcal{R}), \quad L < N.$$

Proof. The exact solution $u \in \mathcal{P}_{L+1}(\mathcal{R})$ and can therefore be represented exactly as $q_n \in \text{span}(\{\varphi_p\}_{p=0}^N)$ (2.5) if and only if $L < N$. The local solution q_n (2.5) is the solution of the weak form (2.6) of the ODE (4.2). However, $f(t) \in \mathcal{P}_L(\mathcal{R}) \subset \mathcal{C}_1(\mathcal{R})$, and $\{\varphi_p\}_{p=0}^N$ is a complete set of functions in $\mathcal{P}_{L+1}(\mathcal{R}) \subseteq \mathcal{P}_N(\mathcal{R})$. Therefore, the solution of the weak form coincides with the solution of the original ODE (4.2). The provable statement follows directly from this. \square

Remark 4.2. Nowhere in Lemma 4.1 is it explicitly used that the nodes $\{\tau_p\}_{p=0}^N$ must be chosen at the roots of Legendre polynomials. Therefore, the Lemma 4.1 is satisfied in the case of left Rado polynomials. In the case of right Rado polynomials, the right node $\tau_N = 1$, so this Lemma can be weakened. As a consequence of (2.15), the local solution at $q_n(1)$ coincides with the solution u_{n+1} at the node t_{n+1} obtained by the Gauss-Rado quadrature formula, similar to (2.8), that is exact for $\mathcal{P}_{2N}(\mathcal{R})$, so the local solution will be exact for an ODE (4.2) with $f(t) \in \mathcal{P}_N(\mathcal{R})$, i.e. $L \leq N$.

Remark 4.3. Following the logic of the previous Remark 4.2, it may seem that in the case of left Rado polynomials the weakening of the Lemma 4.1 should also be fulfilled, since in this case there is always the left node $\tau_0 = 0$, and the initial condition $\mathbf{q}_n(0) = \mathbf{u}_n$ is defined. However, the initial condition is defined precisely in the sense of the weak form (2.6) of the ODE system (1.1), and is used in the integration by parts in the derivation of (2.10) from (2.6). A direct calculation shows:

$$(4.3) \quad \begin{aligned} \mathbf{q}_n(0) &= \sum_{p=0}^N \hat{\mathbf{q}}_{n,p} \psi_p = \mathbf{u}_n + \Delta t_n \sum_{q=0}^N \left[\sum_{p=0}^N a_{pq} \psi_p \right] \mathbf{F}(\hat{\mathbf{q}}_{n,q}, t(\tau_q)), \\ \tilde{w}_q &= \sum_{p=0}^N a_{pq} \psi_p = \sum_{p=0}^N \sum_{r=0}^N [\kappa^{-1}]_{pr} w_r \delta_{rq} \psi_p = w_q \sum_{p=0}^N [\kappa^{-1}]_{pq} \psi_p, \end{aligned}$$

where vector $\tilde{\mathbf{w}} = \|\tilde{w}_q\| \neq 0$ due to $\psi = \|\psi_p\| \neq 0$ and non-degeneracy of matrix κ^{-1} , therefore $\mathbf{q}_n(0) \neq \mathbf{u}_n$ in the general case $\mathbf{F} \neq 0$. Therefore, in the case of left Rado polynomials, weakening Lemma 4.1 is not admissible.

Remark 4.4. In the case of classical GL methods, the Lemma 4.1 can also be weakened to the condition $f(t) \in \mathcal{P}_N(\mathcal{R})$, due to condition $a_{pq} = \int_0^{\tau_p} \varphi_q(\tau) d\tau$.

LEMMA 4.5. $C(N)$ (4.1) is satisfied for the IRK-GL-ADER-DG method.

Proof. The proof is based on the meaning of the simplifying condition $C(L)$ (see [16]) and Lemma 4.1. The simplifying condition $C(L)$ means that $q_{n,p}$ are the values of exact solution of the ODE (4.2) at quadrature points $t_n + \tau_p \Delta t_n$ in discretization domain Ω_n . Note that if and only if the $\mathbf{q}_{n,p}$ are exact solutions at quadrature points and $N > L$, then the local solution \mathbf{q} is an exact solution. Lemma 4.1 shows that \mathbf{q} is exact solution only in case $L < N$, and in case $L \geq N$ the local solution \mathbf{q} is not an exact solution. Therefore, in case $L < N$, the values $\mathbf{q}_{n,p}$ are exact solutions at quadrature points, and in case $L \geq N$ they are not. This proves $C(N)$. \square

Alternative proof of Lemma 4.5. The proof of this lemma is based on the transformation of the simplifying condition $C(N)$:

$$(4.4) \quad \sum_{q=0}^N a_{pq} \tau_q^r = \frac{\tau_p^{r+1}}{r+1}, \quad 0 \leq p \leq N, \quad 0 \leq r \leq N-1.$$

Substituting the parameters of ADER-DG method into $C(N)$ leads to the expression:

$$(4.5) \quad w_p \tau_p^r = \sum_{q=0}^N \frac{\kappa_{pq}}{w_p} \frac{\tau_q^{r+1}}{r+1} = \sum_{q=0}^N \left[\psi_p \psi_q + \int_0^1 \varphi_p(\tau) \frac{d\varphi_q(\tau)}{d\tau} d\tau \right] \frac{\tau_q^{r+1}}{r+1},$$

where for each term the following transformations are performed:

$$(4.6) \quad \sum_{q=0}^N \frac{\tau_q^{r+1}}{r+1} \psi_p \psi_q = \frac{\psi_p}{r+1} \sum_{q=0}^N \tau_q^{r+1} \psi_q = \frac{\psi_p}{r+1} \cdot (0)^{r+1} = 0,$$

$$\begin{aligned} \sum_{q=0}^N \frac{\tau_q^{r+1}}{r+1} \int_0^1 \varphi_p(\tau) \frac{d\varphi_q(\tau)}{d\tau} d\tau &= \int_0^1 \frac{\varphi_p(\tau)}{r+1} \frac{d}{d\tau} \left[\sum_{q=0}^N \tau_q^{r+1} \varphi_q(\tau) \right] d\tau \\ &= \left| \tau^s = \sum_{q=0}^N \tau_q^s \varphi_q(\tau), \quad 0 \leq s \leq N \right| = \int_0^1 \frac{\varphi_p(\tau)}{r+1} \frac{d(\tau^{r+1})}{d\tau} d\tau = \int_0^1 \tau^r \varphi_p(\tau) d\tau = w_p \tau_p^r. \end{aligned}$$

Substituting the transformed terms into the original expression turns it into an identity, which proves the fulfillment of the simplifying condition $C(N)$. \square

Remark 4.6. In the case of right Rado polynomials, following Remark 4.2, the Lemma 4.1 can be weakened, which leads to the fulfillment of the simplifying condition $C(N+1)$, which is known [16, 26].

Remark 4.7. The $r = 0$ in $C(N)$ corresponds to the relation: $\sum_{q=0}^N a_{pq} = \tau_p$.

LEMMA 4.8. $D(N)$ (4.1) is satisfied for the IRK-GL-ADER-DG method.

Proof. The proof of this lemma is based on the transformation of the simplifying condition $D(N)$:

$$(4.7) \quad \sum_{q=0}^N w_q a_{qp} \tau_q^r = \frac{w_p}{r+1} (1 - \tau_p^{r+1}), \quad 0 \leq p \leq N, \quad 0 \leq r \leq N-1.$$

Substituting the parameters of ADER-DG method (2.12), (2.14) into $D(N)$ leads to the following expression:

$$(4.8) \quad w_p \tau_p^r = \sum_{q=0}^N \frac{\kappa_{qp}}{w_q} \frac{w_q}{r+1} (1 - \tau_q^{r+1}) = \sum_{q=0}^N \left[\psi_q \psi_p + \int_0^1 \varphi_q(\tau) \frac{d\varphi_p(\tau)}{d\tau} d\tau \right] \frac{1 - \tau_q^{r+1}}{r+1},$$

where for each term the following transformations are performed:

$$(4.9) \quad \begin{aligned} \sum_{q=0}^N \frac{\psi_q \psi_p}{r+1} &= \frac{\psi_p}{r+1} \sum_{q=0}^N \psi_q = \frac{\psi_p}{r+1}, \\ \sum_{q=0}^N \frac{\tau_q^{r+1}}{r+1} \psi_q \psi_p &= \frac{\psi_p}{r+1} \sum_{q=0}^N \tau_q^{r+1} \psi_q = \frac{\psi_p}{r+1} \cdot (0)^{r+1} = 0, \\ \sum_{q=0}^N \int_0^1 \frac{\varphi_q(\tau)}{r+1} \frac{d\varphi_p(\tau)}{d\tau} d\tau &= \frac{1}{r+1} \int_0^1 \left[\sum_{q=0}^N \varphi_q(\tau) \right] \frac{d\varphi_p(\tau)}{d\tau} d\tau = \frac{\tilde{\psi}_p - \psi_p}{r+1}, \\ \sum_{q=0}^N \frac{\tau_q^{r+1}}{r+1} \int_0^1 \varphi_q(\tau) \frac{d\varphi_p(\tau)}{d\tau} d\tau &= \frac{1}{r+1} \int_0^1 \left[\sum_{q=0}^N \tau_q^{r+1} \varphi_q(\tau) \right] \frac{d\varphi_p(\tau)}{d\tau} d\tau \\ (4.10) \quad &= \frac{1}{r+1} \int_0^1 \tau^{r+1} \frac{d\varphi_p(\tau)}{d\tau} d\tau = \frac{\tau^{r+1} \varphi_p(\tau)}{r+1} \Big|_0^1 - \int_0^1 \tau^r \varphi_p(\tau) d\tau = \frac{\tilde{\psi}_p}{r+1} + w_p \tau_p^r. \end{aligned}$$

Substituting the transformed terms into the original expression turns it into identity:

$$(4.11) \quad w_p \tau_p^r = \frac{\psi_p}{r+1} - 0 + \frac{\tilde{\psi}_p - \psi_p}{r+1} - \frac{\tilde{\psi}_p}{r+1} + w_p \tau_p^r = w_p \tau_p^r,$$

which proves the fulfillment of the simplifying condition $D(N)$. \square

THEOREM 4.9. *The approximation order of the IRK-GL-ADER-DG method is $p_{RK} = 2N + 1$.*

Proof. The nodes $\{\tau_p\}_{p=0}^N$ and weights $\{w_p\}_{p=0}^N$ of the quadrature formula (2.8) ensure (see Lemma 3.3.1 in book [16]) that $B(2N+2)$ is satisfied. Lemmas 4.5 and 4.8 prove the satisfaction of $C(N)$ and $D(N)$, respectively. The famous Butcher's theorem predicts the implication:

$$(4.12) \quad B(2N+2) \wedge C(N) \wedge D(N) \Rightarrow p_{RK} = 2N + 1,$$

in terms of the parameters of the ADER-DG method — $s = N + 1$. \square

COROLLARY 4.10. *The IRK-GL-ADER-DG method is equivalent to the original ADER-DG method, and the numerical solution $\{\mathbf{u}_n\}$ of the RK method corresponds to the numerical solution $\{\mathbf{u}_n\}$ (2.14) obtained by the ADER-DG method, therefore the approximation order for the solution at the nodes $\{\mathbf{u}_n\}$ is also equal $p_G = 2N + 1$ — superconvergence is observed.*

Remark 4.11. The Corollary 4.10 rigorously proves the results of the work [34].

The approximation order $p_{RK} = 2N + 1$ of the IRK-GL-ADER-DG method is one unit less than the approximation order $2N + 2$ of the classical GL method.

COROLLARY 4.12. *The IRK-GL-ADER-DG method is not a collocation method according to Theorem 7.7 in [26], since it has the convergence order $p_{\text{RK}} > s$ and the simplifying condition $C(N+1)$ is not satisfied.*

5. Local solution and subgrid resolution. DG methods, and ADER-DG in particular, have the ability to obtain a numerical solution with subgrid resolution, which was noted in [2–7, 34, 36]. The ADER-DG method is equivalent to the IRK-GL-ADER-DG method, which is not a collocation method, so Theorem 7.9 in [26] cannot be used directly for it.

LEMMA 5.1. *The local solution \mathbf{q}_n (2.5) of the ADER-DG method has an approximation order $p = N + 1$ in \mathcal{L}_∞ -norm on each discretization domain Ω_n :*

$$(5.1) \quad \exists C_n \in \mathcal{R}_+ : \|\mathbf{q}_n - \mathbf{u}\|_{\mathcal{L}_\infty} \triangleq \sup_{t \in \Omega_n} |\mathbf{q}_n(t) - \mathbf{u}(t)| < C_n \cdot \Delta t_n^{N+1}.$$

Proof. The local solution \mathbf{q}_n is the Lagrange interpolation polynomial of degree N (2.5) whose coefficients $\{\hat{\mathbf{q}}_p\}_{p=0}^N$ are the solution of the system of equations (2.12), where \mathbf{u}_n is known with the approximation order $p_{\text{RK}} = 2N + 1$. The exact solution of the ODE system (1.1) in domain Ω_n with the initial condition $\tilde{\mathbf{u}}(t_n) = \mathbf{u}_n$ is denoted as $\tilde{\mathbf{u}} : \Omega_n \rightarrow \mathcal{R}^D$. If $\mathbf{F}(\mathbf{u}, t)$ is a sufficiently smooth function, then

$$(5.2) \quad \exists A_n \in \mathcal{R}_+ : |\tilde{\mathbf{u}}(t) - \mathbf{u}(t)| < A_n |\tilde{\mathbf{u}}(t_n) - \mathbf{u}(t_n)| < A_n C_{\text{app}} \Delta t_n^{2N+2},$$

where C_{app} is the approximation constant of the IRK-GL-ADER-DG method, and $2N + 2$ in the exponent is associated with the approximation order $p_{\text{RK}} = 2N + 1$ at one step $\varepsilon = O(\Delta t_n^{p_{\text{RK}}+1})$, expressed through the local truncation error ε . The error estimate for the Lagrange interpolation polynomial can be presented in the form:

$$(5.3) \quad |\mathbf{q}_n(t) - \tilde{\mathbf{u}}(t)| \leq \frac{\Delta t_n^{N+1}}{(N+1)!} \max_{t \in \Omega_n} \left| \frac{d^{N+1} \tilde{\mathbf{u}}(t)}{dt^{N+1}} \right| \equiv B_n \Delta t_n^{N+1},$$

which is also applicable for sufficiently smooth functions $\mathbf{F}(\mathbf{u}, t)$ due to the Lemma 4.1. As a result of applying the norm property, the following expression is obtained:

$$(5.4) \quad \begin{aligned} |\mathbf{q}_n(t) - \mathbf{u}(t)| &\leq |\mathbf{q}_n(t) - \tilde{\mathbf{u}}(t)| + |\tilde{\mathbf{u}}(t) - \mathbf{u}(t)| \\ &\leq B_n \Delta t_n^{N+1} + A_n C_{\text{app}} \Delta t_n^{2N+2} \equiv O(\Delta t_n^{N+1}), \end{aligned}$$

where the initial provable assumption follows. \square

THEOREM 5.2. *The local solution \mathbf{u}_L (2.4) of the ADER-DG method has an approximation order $p_L = N + 1$ in \mathcal{L}_∞ -norm:*

$$(5.5) \quad \exists C \in \mathcal{R}_+ : \|\mathbf{u}_L - \mathbf{u}\|_{\mathcal{L}_\infty} \triangleq \text{ess sup}_{t \in \Omega} |\mathbf{u}_L(t) - \mathbf{u}(t)| < C \cdot \Delta t^{N+1}, \quad \Delta t = \max_n \Delta t_n.$$

Proof. Taking into account the fact of discretization of the domain of definition Ω by a finite set of $\{\Omega_n\}$ and in the case $\mathbf{u} \in \mathcal{C}_0(\Omega)$, the following expression is obtained:

$$(5.6) \quad \text{ess sup}_{t \in \Omega} |\mathbf{u}_L(t) - \mathbf{u}(t)| = \max_n \sup_{t \in \Omega_n} |\mathbf{u}_L(t) - \mathbf{u}(t)| = \max_n \sup_{t \in \Omega_n} |\mathbf{q}_n(t) - \mathbf{u}(t)|.$$

Following the Lemma 5.1, the following estimate is obtained:

$$(5.7) \quad \max_n \sup_{t \in \Omega_n} |\mathbf{q}_n(t) - \mathbf{u}(t)| < \max_n C_n \cdot \Delta t_n^{N+1} < C \cdot \Delta t^{N+1}, \quad C > \max_n C_n,$$

where the initial provable assumption follows. \square

COROLLARY 5.3. *The local solution \mathbf{u}_L at the nodal points $t_n + \tau_p \Delta t_n$ coincides with the coefficients $\{\hat{\mathbf{q}}_{n,p}\}$, so the approximation order of the local solution at the nodal points $\{\hat{\mathbf{q}}_{n,p}\}$ is also $p_L = N + 1$.*

THEOREM 5.4. *The local solution \mathbf{u}_L (2.4) of the ADER-DG method has an approximation order $p_L = N + 1$ in \mathcal{L}_q -norm:*
(5.8)

$$\exists C_q \in \mathcal{R}_+ : \|\mathbf{u}_L - \mathbf{u}\|_{\mathcal{L}_q} \triangleq \left[\int_{\Omega} |\mathbf{u}_L(t) - \mathbf{u}(t)|^q dt \right]^{1/q} < C_q \cdot \Delta t^{N+1}, \quad \Delta t = \max_n \Delta t_n.$$

Proof. Using the inequality $|\mathbf{f}| < \|\mathbf{f}\|_{\mathcal{L}_\infty}$ in the assumption:

$$(5.9) \quad \int_{\Omega} |\mathbf{u}_L(t) - \mathbf{u}(t)|^q dt \leq \int_{\Omega} \|\mathbf{u}_L(t) - \mathbf{u}(t)\|_{\mathcal{L}_\infty}^q dt = \|\mathbf{u}_L(t) - \mathbf{u}(t)\|_{\mathcal{L}_\infty}^q \cdot |\Omega|,$$

where $|\Omega| = t_f - t_0$, and according to the Theorem 5.2, the estimate is obtained:

$$(5.10) \quad \|\mathbf{u}_L - \mathbf{u}\|_{\mathcal{L}_q} \leq \left[\frac{1}{|\Omega|} \|\mathbf{u}_L(t) - \mathbf{u}(t)\|_{\mathcal{L}_\infty}^q \right]^{1/q} \leq \frac{C}{|\Omega|^{1/q}} \cdot \Delta t^{N+1} \equiv C_q \cdot \Delta t^{N+1},$$

where the initial provable assumption follows. \square

Remark 5.5. Theorems 5.2 and 5.4 rigorously proves the results of the work [34].

6. Linear and nonlinear stability. The analysis of nonlinear stability of the IRK-GL-ADER-DG method is based on the study of the properties of non-negative definiteness of matrices μ , \mathbf{Q} and \mathbf{M} [16]:

$$(6.1) \quad \mathbf{Q} = \mu\alpha + \alpha^T \mu - \alpha^T \mathbf{w} \mathbf{w}^T \alpha, \quad \mathbf{M} = a^T \mathbf{Q} a = \mu a + a^T \mu - \mathbf{w} \mathbf{w}^T,$$

where $\mathbf{w} = [w_0 \dots w_N]^T$ and $\alpha = a^{-1} = [\kappa^{-1} \mu]^{-1} = \mu^{-1} \kappa$. Matrix μ is positive definite, since it is diagonal and contains $w_p > 0$ on the diagonal.

LEMMA 6.1. *Matrix $\mathbf{Q} = \boldsymbol{\psi} \boldsymbol{\psi}^T$, where $\boldsymbol{\psi} = \|\boldsymbol{\psi}_p\| \neq 0$.*

Proof. The proof is based on the element-by-element description of the matrix $\mathbf{Q} = \|Q_{pq}\|$ and the use of the definitions of matrices κ and μ (2.11):

$$(6.2) \quad Q_{pq} = w_p \alpha_{pq} + w_q \alpha_{qp} - \sum_{i=0}^N \sum_{j=0}^N \alpha_{ip} w_i w_j \alpha_{jq} = \kappa_{pq} + \kappa_{qp} - \sum_{i=0}^N \sum_{j=0}^N \kappa_{ip} \kappa_{jq}.$$

Then each term is studied and folded separately:

$$\kappa_{pq} + \kappa_{qp} = \tilde{\psi}_p \tilde{\psi}_q + \tilde{\psi}_q \tilde{\psi}_p - \int_0^1 \left[\frac{d\varphi_p(\tau)}{d\tau} \varphi_q(\tau) + \frac{d\varphi_q(\tau)}{d\tau} \varphi_p(\tau) \right] d\tau = \tilde{\psi}_p \tilde{\psi}_q + \psi_p \psi_q,$$

$$\begin{aligned}
\sum_{i=0}^N \sum_{j=0}^N \kappa_{ip} \kappa_{jq} &= \sum_{i=0}^N \sum_{j=0}^N \tilde{\psi}_i \tilde{\psi}_p \tilde{\psi}_j \tilde{\psi}_q + \sum_{i=0}^N \sum_{j=0}^N \int_0^1 \frac{d\varphi_i(\tau)}{d\tau} \varphi_p(\tau) d\tau \cdot \int_0^1 \frac{d\varphi_j(\tau)}{d\tau} \varphi_q(\tau) d\tau \\
&- \sum_{i=0}^N \sum_{j=0}^N \tilde{\psi}_i \tilde{\psi}_p \cdot \int_0^1 \frac{d\varphi_j(\tau)}{d\tau} \varphi_q(\tau) d\tau - \sum_{i=0}^N \sum_{j=0}^N \int_0^1 \frac{d\varphi_i(\tau)}{d\tau} \varphi_p(\tau) d\tau \cdot \tilde{\psi}_j \tilde{\psi}_q \\
&= \left[\sum_{i=0}^N \tilde{\psi}_i \right] \left[\sum_{j=0}^N \tilde{\psi}_j \right] \tilde{\psi}_p \tilde{\psi}_q + \int_0^1 \frac{d}{d\tau} \left[\sum_{i=0}^N \varphi_i(\tau) \right] \varphi_p(\tau) d\tau \cdot \int_0^1 \frac{d}{d\tau} \left[\sum_{j=0}^N \varphi_j(\tau) \right] \varphi_q(\tau) d\tau \\
&- \left[\sum_{i=0}^N \tilde{\psi}_i \right] \tilde{\psi}_p \cdot \int_0^1 \frac{d}{d\tau} \left[\sum_{j=0}^N \varphi_j(\tau) \right] \varphi_q(\tau) d\tau - \int_0^1 \frac{d}{d\tau} \left[\sum_{i=0}^N \varphi_i(\tau) \right] \varphi_p(\tau) d\tau \cdot \left[\sum_{j=0}^N \tilde{\psi}_j \right] \tilde{\psi}_q \\
&= \tilde{\psi}_p \tilde{\psi}_q.
\end{aligned}$$

The final substitution of the folded expressions of the terms into the original expression leads to the result $Q_{pq} = \tilde{\psi}_p \tilde{\psi}_q$, which is the result for matrix Q being proven. \square

LEMMA 6.2. *Matrices Q and M are non-negative definite.*

Proof. The dyadic matrix \mathbf{ab}^T , where $\mathbf{a} \neq \mathbf{0}$, $\mathbf{b} \neq \mathbf{0}$, has all zero eigenvalues except one $\lambda = \mathbf{a}^T \mathbf{b}$. In the case of dyadic square \mathbf{aa}^T , where $\mathbf{a} \neq \mathbf{0}$, $\lambda = \mathbf{a}^T \mathbf{a} = |\mathbf{a}|^2 > 0$, so dyadic squares are non-negative definite. Matrix Q is dyadic square by Lemma 6.1, so it is non-negative definite. Matrix $M = a^T Q a = a^T \boldsymbol{\psi} \boldsymbol{\psi}^T a = (a^T \boldsymbol{\psi})(a^T \boldsymbol{\psi})^T$, and is also dyadic square, so it is non-negative definite, since a is not degenerate and $\boldsymbol{\psi} = \|\boldsymbol{\psi}_p\| \neq 0$. \square

COROLLARY 6.3. $\lambda_Q = |\boldsymbol{\psi}|^2 = \sum_{p=0}^N \tilde{\psi}_p^2 > 0$ and $\lambda_M = |a^T \boldsymbol{\psi}|^2 > 0$ are only non-negative eigenvalues of Q and M , respectively.

THEOREM 6.4. *The IRK-GL-ADER-DG method is algebraically stable.*

Proof. The matrix M (6.1) is non-negative definite by Lemma 6.2, and matrix μ (2.11) is positive definite, so the IRK-GL-ADER-DG method is algebraically stable, by Definition 4.2.1 in [16]. \square

COROLLARY 6.5. *The IRK-GL-ADER-DG method is BN-stable by the Theorem 4.2.2 in [16], and B-stable as a special case.*

RK methods are usually defined by matrix a , so the stability analysis is carried out not by Q , but by M . It is more convenient to use matrix Q for the IRK-GL-ADER-DG method, since it is more convenient to use a^{-1} containing κ , not κ^{-1} .

Remark 6.6. Theorem 4.6.1 in [16] shows $\text{rank}(M) \leq 2s - p_{\text{RK}} = 1$, and the Lemma 6.2 leads to result $\text{rank}(M) = 1$, since the matrix M is dyadic.

Remark 6.7. According to Lemma 6.2, by Theorem 4.1.3 in [16], B -stability of the IRK-GL-ADER-DG method can be proven by the non-negative definiteness of Q .

THEOREM 6.8. *The IRK-GL-ADER-DG method is AN-stable.*

Proof. Legendre polynomials \tilde{P}_{N+1} do not have multiple roots τ_p , so all abscissas τ_p are different: $\tau_p = \tau_q$ if and only if $p = q$, hence the IRK-GL-ADER-DG method is non-confluent. By Theorem 4.3.5 in [16] any non-confluent algebraically stable method is AN-stable. This proves the AN-stability of the IRK-GL-ADER-DG method. \square

COROLLARY 6.9. *The IRK-GL-ADER-DG method is A-stable as a special case.*

THEOREM 6.10. *The stability function $R(z)$ of the IRK-GL-ADER-DG method is the $(N, N+1)$ -Padé approximation $R_{N,N+1}(z)$ of $\exp(z)$.*

Proof. The stability function $R(z)$ is defined by the expression:

$$(6.3) \quad R(z) = 1 + \mathbf{w}^T z [\mathbf{I} - za]^{-1} \mathbf{1} = \frac{\mathbf{I} - za + z\mathbf{1}\mathbf{w}^T}{\mathbf{I} - za} = \frac{P_{N,N+1}(z)}{R_{N,N+1}(z)}.$$

The matrix $a = \kappa^{-1} \cdot \mu$ in the denominator is invertible and $\text{rank}(a) = N+1$. The denominator of $R(z)$ is a polynomial $R_{N,N+1}(z)$ of degree N . To determine the form of the Padé approximation, it is necessary to calculate the rank of the matrix $a - \mathbf{1}\mathbf{w}^T$ in the numerator. The rank can be calculated through the dimension of the null space of the matrix, defined by the linear system:

$$(6.4) \quad [a - \mathbf{1}\mathbf{w}^T] \mathbf{c} = \mathbf{0}, \Rightarrow a\mathbf{c} = \mathbf{1}\mathbf{w}^T \mathbf{c}, \Rightarrow \mathbf{c} = a^{-1} \mathbf{1}\mathbf{w}^T \mathbf{c} = \mu^{-1} \kappa \mathbf{1}\mathbf{w}^T \mathbf{c},$$

which in component-wise notation takes the form:

$$(6.5) \quad c_p = \sum_{q=0}^N \sum_{r=0}^N \frac{1}{w_p} \kappa_{pr} w_q c_q, \Rightarrow w_p c_p = \sum_{q=0}^N \sum_{r=0}^N \kappa_{pr} w_q c_q = \psi_p \sum_{q=0}^N w_q c_q,$$

which after replacing the desired vector $\mathbf{x} = \|x_p\|$, with $x_p = w_p c_p$, is transformed to:

$$(6.6) \quad \sum_{q=0}^N [\delta_{pq} - \psi_p] x_q = 0, \Rightarrow [\mathbf{I} - \psi \mathbf{1}^T] \mathbf{x} = \mathbf{0}, \quad \psi = \|\psi_p\|,$$

which leads to $\text{rank}(a - \mathbf{1}\mathbf{w}^T) = \text{rank}(\mathbf{I} - \psi \mathbf{1}^T)$. From considerations $\text{rank}(\psi \mathbf{1}^T) = 1$ and $\text{rank}(\mathbf{I}) = N+1$ it follows that $N \leq \text{rank}(\mathbf{I} - \psi \mathbf{1}^T) \leq N+1$, therefore the rank N or $N+1$ is associated with the invertibility of the matrix $\mathbf{I} - \psi \mathbf{1}^T$. According to the Sherman-Morrison formula, such a matrix is irreversible if and only if $\psi^T \mathbf{1} = 1$, i.e. $\sum_{p=0}^N \psi_p = 1$, which is satisfied. Therefore $\text{rank}(\mathbf{I} - \psi \mathbf{1}^T) = N$, and $\text{rank}(a - \mathbf{1}\mathbf{w}^T) = N$. Therefore the numerator of $R(z)$ is a polynomial $P_{N,N+1}(z)$ of degree $N-1$. It follows that $R(z)$ is the $(N, N+1)$ -Padé approximation $R_{N,N+1}(z)$ of $\exp(z)$. \square

Symbolic calculations in the `Maple` for degrees $N = 1, \dots, 6$ showed that the function $R(z)$ coincides with the $(N, N+1)$ -Padé approximation of $\exp(z)$. Numerical calculations using module `mpmath` of the `python` programming language, with an arithmetic precision constant `mpmath.mp.dps = 1000`, also confirmed this result for degrees $N = 1, \dots, 75$ with accuracy $\approx 10^{-946} - 10^{-1002}$.

COROLLARY 6.11. *The $(N, N+1)$ -Padé approximation $R_{N,N+1}(z)$ of $\exp(z)$ is A -admissible function by Theorem 3.4.8 in [16], so the Theorem 6.10 provides an alternative proof of the A -stability of the IRK-GL-ADER-DG method.*

COROLLARY 6.12. *By Theorem 3.11 in [27], the residual term of the $R_{N,N+1}(z)$ is $\exp(z) - R_{N,N+1}(z) = O(z^{2N+2})$, so the approximation order of the IRK-GL-ADER-DG method $p_{\text{RK}} = 2N+1$, which is an alternative proof of Theorem 4.9.*

THEOREM 6.13. *The IRK-GL-ADER-DG method is L -stable.*

Proof. The IRK-GL-ADER-DG method is A -stable, and the stability function $R(z)$ has asymptotics $|z|^{-1}$, $z \in \mathcal{C}$, in domain $z \rightarrow \infty$ as $(N, N+1)$ -Padé approximation, so the IRK-GL-ADER-DG method is L -stable. \square

Remark 6.14. The classical GL method is only A -stable, but not L -stable. Decreasing the approximation order “led to” an increase in the stability.

COROLLARY 6.15. *The IRK-GL-ADER-DG method is equivalent to the original ADER-DG method, therefore, the ADER-DG method is A -stable, AN -stable, L -stable, algebraically stable, B -stable and BN -stable.*

A -stability and L -stability of the ADER-DG method were numerically demonstrated in [34], and in this paper, these and other types of numerical stability are proven.

7. Computational results. The Section presents two examples of using the ADER-DG method to solve ODE systems. The first example is a classical one-dimensional harmonic oscillator described by a linear ODE:

$$(7.1) \quad \ddot{x} + x = 0, \quad x(0) = 1, \quad \dot{x}(0) = 0, \quad t \in [0, 4\pi],$$

and the second example is a mathematical pendulum described by a nonlinear ODE:

$$(7.2) \quad \ddot{\phi} + \sin(\phi) = 0, \quad \phi(0) = \frac{\pi}{2}, \quad \dot{\phi}(0) = 0, \quad t \in [0, 10].$$

Exact analytical solutions of these ODE systems are obtained by trivial integration.

The solution at grid nodes \mathbf{u}_n , the local solution \mathbf{u}_L (2.4) in space between nodes $\{\Omega_n\}$, and the local solution $\mathbf{u}_L(t_{n,p})$ at nodal points $\{t_n + \tau_p \Delta t\}$ are calculated and analyzed. The local error $\varepsilon : \Omega \rightarrow \mathcal{R}_+$ is calculated using the uniform norm of the solution vector \mathbf{u} : $\varepsilon(t) = |\mathbf{u}(t) - \mathbf{u}^{\text{ex}}(t)|$, where \mathbf{u}^{ex} is the exact solution.

The calculation of empirical convergence orders p is carried out separately for each presented type of numerical solution, and is based on a power approximation of the dependence of global errors $e(\Delta t) \propto \Delta t^p$ on the discretization step Δt . The domain of definition Ω was discretized into M discretization domains $\{\Omega_n\}$, with a discretization step $\Delta t = (t_f - t_0)/M$. The following 14 types of global errors e :

$$\begin{aligned} e_{L_1}^n &= \sum_{n=0}^M \Delta t_n |\mathbf{u}_n - \mathbf{u}^{\text{ex}}(t_n)|, & e_{L_1}^{l,q} &= \sum_{n=0}^M \sum_{p=0}^N \Delta t_{n,p} |\mathbf{u}_L(t_{n,p}) - \mathbf{u}^{\text{ex}}(t_{n,p})|, \\ e_{L_2}^n &= \left[\sum_{n=0}^M \Delta t_n |\mathbf{u}_n - \mathbf{u}^{\text{ex}}(t_n)|^2 \right]^{\frac{1}{2}}, & e_{L_2}^{l,q} &= \left[\sum_{n=0}^M \sum_{p=0}^N \Delta t_{n,p} |\mathbf{u}_L(t_{n,p}) - \mathbf{u}^{\text{ex}}(t_{n,p})|^2 \right]^{\frac{1}{2}}, \\ e_{L_\infty}^n &= \max_{0 \leq n \leq M} |\mathbf{u}_n - \mathbf{u}^{\text{ex}}(t_n)|, & e_{L_\infty}^{l,q} &= \max_{0 \leq n \leq M} \max_{0 \leq p \leq N} |\mathbf{u}_L(t_{n,p}) - \mathbf{u}^{\text{ex}}(t_{n,p})|, \\ e_f^n &= |\mathbf{u}_M - \mathbf{u}^{\text{ex}}(t_f)|, & e_{L_\infty}^l &= \max_{0 \leq n \leq M} \sup_{t \in \Omega_n} |\mathbf{u}_L(t) - \mathbf{u}^{\text{ex}}(t)|, \\ e_{L_1}^l &= \sum_{n=0}^{M-1} \int_{\Omega_n} |\mathbf{u}_L(t) - \mathbf{u}^{\text{ex}}(t)| dt, & e_{L_2}^l &= \left[\sum_{n=0}^{M-1} \int_{\Omega_n} |\mathbf{u}_L(t) - \mathbf{u}^{\text{ex}}(t)|^2 dt \right]^{\frac{1}{2}}, \\ e_{L_1}^{l,n} &= \sum_{n=0}^M \Delta t_n |\mathbf{u}_L(t_n) - \mathbf{u}^{\text{ex}}(t_n)|, & e_{L_2}^{l,n} &= \left[\sum_{n=0}^M \Delta t_n |\mathbf{u}_L(t_n) - \mathbf{u}^{\text{ex}}(t_n)|^2 \right]^{\frac{1}{2}}, \\ e_{L_\infty}^{l,n} &= \max_{0 \leq n \leq M} |\mathbf{u}_L(t_n) - \mathbf{u}^{\text{ex}}(t_n)|, & e_f^{l,n} &= |\mathbf{u}_L(t_f) - \mathbf{u}^{\text{ex}}(t_f)|, \end{aligned}$$

where $t_{n,p} = t_n + \tau_p \Delta t$ is nodal points, $\Delta t_{n,p}$ is distance to the next nodal point or t_f , and 14 corresponding empirical convergence orders p in different norms are selected.

In the implementation of the ADER-DG method, the system of equations (3.2) was solved to calculate $\{\mathbf{k}_p\}$ (for which numerical methods are developed [10, 16, 26, 27]), from which $\{\mathbf{q}_p\}$ are calculated (3.1), unlike [34], where direct system (2.12) of the local DG predictor was solved, although of course the result did not change.

The software implementation of the ADER-DG numerical method is developed in the `python` programming language. The error of the numerical solution becomes very small even on fairly coarse grids. Therefore, floating-point numbers of arbitrary precision are used in the `mpmath` module, and `mpmath.mp.dps = 500` is chosen.

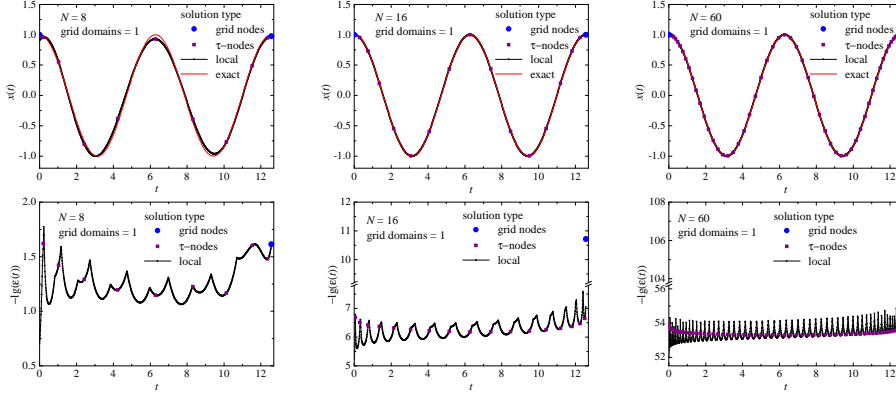


FIG. 1. Numerical solution $x(t)$ and its error $\varepsilon(t)$, as the negative common logarithm $-\lg(\varepsilon(t))$, obtained by the ADER-DG method with $N = 8, 16, 60$ on a grid with one discretization domain for problem (7.1). The red line shows the exact analytical solution for comparison.

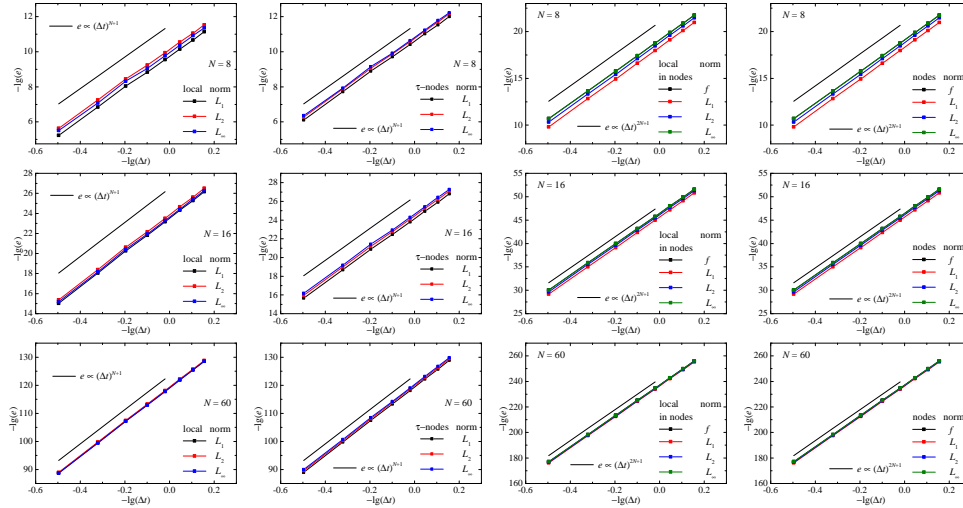


FIG. 2. Dependence of error e on discretization step Δt , as the negative common logarithms, for local solution \mathbf{u}_L in space between nodes $\{\Omega_n\}$, local solution $\mathbf{u}_L(t_n, p)$ at nodal points $\{t_n + \tau_p \Delta t\}$, local solution $\mathbf{u}_L(t_n)$ at grid nodes $\{t_n\}$ and solution at grid nodes \mathbf{u}_n , calculated in norms $\mathcal{L}_1, \mathcal{L}_2, \mathcal{L}_\infty$ and “final” norm, obtained by the ADER-DG method with $N = 8, 16, 60$. Lines represent reference slopes for convergence orders $p_L = N + 1$ and $p_G = 2N + 1$.

Fig. 1 shows a demonstration example of numerical solution of the problem (7.1) obtained on a grid with only one discretization domain, which demonstrates a very

TABLE 1
Empirical orders of convergence p of the Runge-Kutta method based on ADER-DG method for the ODE system (7.1).

N	The numerical solution \mathbf{u}_n at grid nodes				The local solution $\mathbf{u}_L(l)$											
	p_f^n	$p_{L_1}^n$	$p_{L_2}^n$	$p_{L_\infty}^n$	PG	$p_f^{l,n}$	$p_{L_1}^{l,n}$	$p_{L_2}^{l,n}$	$p_{L_\infty}^{l,n}$	$p_{L_1}^l$	$p_{L_2}^l$	$p_{L_\infty}^l$	$p_{L_1}^{l,q}$	$p_{L_2}^{l,q}$	$p_{L_\infty}^{l,q}$	p_L
1	2.02	2.30	2.24	2.02	3	2.02	2.30	2.24	2.02	2.00	1.96	1.77	2.06	2.00	1.71	2
2	4.57	4.76	4.73	4.57	5	4.57	4.76	4.73	4.57	3.29	3.19	2.76	3.33	3.42	3.64	3
3	6.75	6.93	6.90	6.75	7	6.75	6.93	6.90	6.75	4.06	3.99	3.88	4.02	4.03	4.19	4
4	8.82	9.00	8.97	8.82	9	8.82	9.00	8.97	8.82	5.00	4.96	4.90	4.96	4.97	4.99	5
5	10.86	11.04	11.01	10.86	11	10.86	11.04	11.01	10.86	6.00	5.97	5.91	5.97	5.97	5.97	6
6	12.88	13.06	13.03	12.88	13	12.88	13.06	13.03	12.88	6.99	6.97	6.92	6.98	6.98	6.95	7
7	14.90	15.08	15.05	14.90	15	14.90	15.08	15.05	14.90	7.99	7.98	7.93	7.98	7.98	7.95	8
8	16.91	17.09	17.06	16.91	17	16.91	17.09	17.06	16.91	8.99	8.98	8.94	8.99	8.99	8.95	9
9	18.92	19.10	19.07	18.92	19	18.92	19.10	19.07	18.92	10.00	9.98	9.94	9.99	9.99	9.96	10
10	20.93	21.11	21.08	20.93	21	20.93	21.11	21.08	20.93	11.00	10.99	10.95	10.99	10.99	10.96	11
11	22.94	23.12	23.09	22.94	23	22.94	23.12	23.09	22.94	12.00	11.99	11.95	12.00	11.99	11.96	12
12	24.94	25.12	25.09	24.94	25	24.94	25.12	25.09	24.94	13.00	12.99	12.95	13.00	13.00	12.96	13
13	26.95	27.13	27.10	26.95	27	26.95	27.13	27.10	26.95	14.00	13.99	13.95	14.00	14.00	13.96	14
14	28.95	29.13	29.10	28.95	29	28.95	29.13	29.10	28.95	15.00	14.99	14.96	15.00	15.00	14.96	15
15	30.95	31.14	31.10	30.95	31	30.95	31.14	31.10	30.95	16.00	16.00	15.96	16.00	16.00	15.96	16
16	32.96	33.14	33.11	32.96	33	32.96	33.14	33.11	32.96	17.00	17.00	16.96	17.00	17.00	16.96	17
17	34.96	35.14	35.11	34.96	35	34.96	35.14	35.11	34.96	18.00	18.00	17.96	18.00	18.00	17.97	18
18	36.96	37.14	37.11	36.96	37	36.96	37.14	37.11	36.96	19.01	19.00	18.96	19.00	19.00	18.97	19
19	38.96	39.15	39.11	38.96	39	38.96	39.15	39.11	38.96	20.01	20.00	19.96	20.01	20.00	19.97	20
20	40.96	41.15	41.12	40.96	41	40.96	41.15	41.12	40.96	21.01	21.00	20.96	21.01	21.00	20.97	21
21	42.97	43.15	43.12	42.97	43	42.97	43.15	43.12	42.97	22.01	22.00	21.96	22.01	22.01	21.97	22
22	44.97	45.15	45.12	44.97	45	44.97	45.15	45.12	44.97	23.01	23.00	22.97	23.01	23.01	22.97	23
23	46.97	47.15	47.12	46.97	47	46.97	47.15	47.12	46.97	24.01	24.00	23.97	24.01	24.01	23.97	24
24	48.97	49.15	49.12	48.97	49	48.97	49.15	49.12	48.97	25.01	25.00	24.97	25.01	25.01	24.97	25
25	50.97	51.16	51.12	50.97	51	50.97	51.16	51.12	50.97	26.01	26.00	25.97	26.01	26.01	25.97	26
30	60.98	61.16	61.13	60.98	61	60.98	61.16	61.13	60.98	31.01	31.01	30.97	31.01	31.01	30.97	31
35	70.98	71.16	71.13	70.98	71	70.98	71.16	71.13	70.98	36.01	36.01	35.97	36.01	36.01	35.97	36
40	80.98	81.17	81.13	80.98	81	80.98	81.17	81.13	80.98	41.01	41.01	40.97	41.01	41.01	40.97	41
45	90.98	91.17	91.14	90.98	91	90.98	91.17	91.14	90.98	46.01	46.01	45.97	46.01	46.01	45.97	46
50	100.99	101.17	101.14	100.99	101	100.99	101.17	101.14	100.99	51.01	51.01	50.97	51.02	51.02	50.98	51
55	110.99	111.17	111.14	110.99	111	110.99	111.17	111.14	110.99	56.01	56.01	55.97	56.02	56.02	55.98	56
60	120.99	121.17	121.14	120.99	121	120.99	121.17	121.14	120.99	61.01	61.01	60.97	61.01	61.01	60.98	61

TABLE 2
Empirical orders of convergence p of the Runge-Kutta method based on ADER-DG method for the ODE system (7.2).

N	The numerical solution \mathbf{u}_n at grid nodes				The local solution $\mathbf{u}_L(l)$									
	p_f^n	$p_{L_1}^n$	$p_{L_2}^n$	$p_{L_\infty}^n$	pg	$p_f^{l,n}$	$p_{L_1}^{l,n}$	$p_{L_2}^{l,n}$	$p_{L_\infty}^{l,n}$	$p_{L_1}^l$	$p_{L_2}^l$	$p_{L_\infty}^l$	$p_{L_1}^{l,q}$	$p_{L_\infty}^{l,q}$
1	2.79	2.90	2.87	2.73	3	2.79	2.90	2.87	2.73	2.41	2.42	2.13	2.47	2.53
2	4.78	4.86	4.84	4.76	5	4.78	4.86	4.84	4.76	3.09	2.99	2.93	3.07	3.04
3	6.81	6.96	6.93	6.82	7	6.81	6.96	6.93	6.82	3.98	3.96	3.86	3.95	3.96
4	8.66	8.70	8.69	8.60	9	8.66	8.70	8.69	8.60	4.94	4.91	4.84	4.95	4.94
5	10.82	10.97	10.96	10.87	11	10.82	10.97	10.96	10.87	5.97	5.91	5.78	5.98	5.95
6	12.62	12.67	12.63	12.57	13	12.62	12.67	12.63	12.57	6.92	6.91	6.87	6.91	6.94
7	14.69	14.81	14.82	14.73	15	14.69	14.81	14.82	14.73	7.83	7.81	7.68	7.81	7.85
8	16.62	16.74	16.68	16.57	17	16.62	16.74	16.68	16.57	8.97	8.99	8.81	8.97	8.98
9	18.63	18.67	18.73	18.60	19	18.63	18.67	18.73	18.60	9.71	9.66	9.58	9.75	9.77
10	20.44	20.64	20.56	20.42	21	20.44	20.64	20.56	20.42	11.05	11.06	10.92	10.99	10.99
11	22.81	22.77	22.87	22.76	23	22.81	22.77	22.87	22.76	11.61	11.57	11.50	11.70	11.74
12	24.00	24.28	24.19	24.06	25	24.00	24.28	24.19	24.06	13.09	13.09	12.94	12.97	12.95
13	27.14	27.10	27.17	27.10	27	27.14	27.10	27.17	27.10	13.58	13.56	13.48	13.78	13.78
14	27.25	27.57	27.47	27.33	29	27.25	27.57	27.47	27.33	14.95	14.93	14.80	14.83	14.74
15	31.26	31.32	31.33	31.24	31	31.26	31.32	31.33	31.24	15.75	15.69	15.51	15.89	15.87
16	30.47	31.16	31.10	30.89	33	30.47	31.16	31.10	30.89	16.60	16.69	16.64	16.40	16.45
17	35.21	35.36	35.34	35.20	35	35.21	35.36	35.34	35.20	17.97	17.79	17.46	18.05	17.92
18	35.39	35.31	35.36	35.36	37	35.39	35.31	35.36	35.36	18.54	18.58	18.36	18.42	18.35
19	39.12	39.31	39.27	39.15	39	39.12	39.31	39.27	39.15	19.89	19.79	19.35	19.94	19.90
20	39.66	39.38	39.51	39.58	41	39.66	39.38	39.51	39.58	20.69	20.58	20.30	20.59	20.42
21	42.99	43.17	43.14	43.04	43	42.99	43.17	43.14	43.04	21.76	21.74	21.39	21.81	21.84
22	43.66	43.69	43.65	43.56	45	43.66	43.69	43.65	43.56	22.61	22.58	22.29	22.52	22.48
23	46.71	46.87	46.87	46.78	47	46.71	46.87	46.87	46.78	23.72	23.69	23.49	23.80	23.78
24	46.90	47.94	47.84	47.60	49	46.90	47.94	47.84	47.60	24.53	24.55	24.27	24.52	24.51
25	50.07	50.25	50.31	50.34	51	50.07	50.25	50.31	50.34	25.74	25.69	25.50	25.72	25.73
30	59.65	59.82	59.72	59.63	61	59.65	59.82	59.72	59.63	30.53	30.45	30.21	30.57	30.48
35	70.54	71.18	71.05	70.74	71	70.54	71.18	71.05	70.74	35.33	35.22	34.98	35.36	35.42
40	79.33	79.29	79.30	79.18	81	79.33	79.29	79.30	79.18	40.61	40.57	40.32	40.58	40.50
45	90.70	91.16	91.09	90.69	91	90.70	91.16	91.09	90.69	45.16	44.95	44.66	45.22	45.08
50	100.11	100.12	100.20	100.14	101	100.11	100.12	100.20	100.14	50.07	50.26	50.13	50.11	50.23
55	109.24	109.65	109.61	109.58	111	109.24	109.65	109.61	109.58	54.89	54.76	54.53	54.45	54.39
60	120.68	120.59	120.71	120.70	121	120.68	120.59	120.71	120.70	60.74	60.57	60.19	61.08	61.04

high accuracy of the numerical solution. Fig. 2 shows examples of the dependencies of errors e on the discretization step Δt for $N = 8, 16, 60$, with number $M = 4, 6, 8, 10, 12, 14, 16, 18$ of discretization domains. It is evident that the curves $e(\Delta t)$ in the double logarithmic scale are lines $\lg(e(\Delta t)) \propto \lg(\Delta t)$, and their slopes corresponds well to the expected reference values p_G and p_L .

Details of the empirical convergence orders p calculated for problem (7.1) are presented in Table 1 for $N = 1, \dots, 60$. Comparison of the empirical convergence orders p with expected values p_G and p_L shows very good agreement, which demonstrates the applicability of the theory of the ADER-DG method developed in this paper. Similar data on the empirical convergence orders calculated for problem (7.2) are presented in Table 2. These empirical convergence orders p also demonstrate a very good agreement with the expected values p_G and p_L .

8. Conclusion. In conclusion, it should be noted that in this paper a rigorous study of the approximation, convergence and stability of the arbitrary high order ADER-DG method for solving the IVP for an ODE system has been carried out.

It is shown that the ADER-DG method generates a new implicit RK method (3.2), called IRK-GL-ADER-DG, which is similar in its properties to the original ADER-DG method. This RK method has weights and abscissas corresponding to the GL method, but has a different method matrix a .

The approximation orders of the ADER-DG method are calculated. It is proven that the ADER-DG method has an approximation order $p_G = 2N+1$ for the numerical solution in grid nodes, therefore it demonstrates superconvergence. This order is one less than the order of the GL method. It is proved that the local solution obtained by the local DG predictor has the approximation order $p_L = N + 1$.

The linear and nonlinear stability properties of the ADER-DG method are clarified and proved. It is proved that the ADER-DG method is AN -stable, and as a consequence A -stable, and L -stable, in contrast to the GL method. It is proved that the ADER-DG method has the property of nonlinear BN -stability, and as a consequence B -stable, and it is algebraically stable.

Several other relations useful for an application and implementation of the ADER-DG method are proved. The relationship between the ADER-DG method and the RK method it generates with other RK methods, such as Rado methods, is revealed.

Examples of the application of the ADER-DG method for solving the ODE system are presented, which demonstrated good agreement with the expected theoretical results. The empirical results [34] are proven. It is planned to construct a theory of the ADER-DG method as applied to PDE systems based on the developed theory.

Acknowledgments. The author would like to thank A.P. Popova for help in correcting the English text.

REFERENCES

- [1] I. BABUŠKA AND T. STROUBOULIS, *The Finite Element Method and Its Reliability*, Numerical Mathematics and Scientific Computation, Clarendon Press, Oxford, 2001.
- [2] M. BACCOUCH, *Analysis of a posteriori error estimates of the discontinuous Galerkin method for nonlinear ordinary differential equations*, Appl. Numer. Math., 106 (2016), pp. 129–153.
- [3] M. BACCOUCH, *A posteriori error estimates and adaptivity for the discontinuous Galerkin solutions of nonlinear second-order initial-value problems*, Appl. Numer. Math., 121 (2017), pp. 18–37.
- [4] M. BACCOUCH, *Superconvergence of the discontinuous Galerkin method for nonlinear second-order initial-value problems for ordinary differential equations*, Appl. Numer. Math., 115 (2017), pp. 160–179.

- [5] M. BACCOUCH, *Analysis of optimal superconvergence of the local discontinuous Galerkin method for nonlinear fourth-order boundary value problems*, Numerical Algorithms, 86 (2021), pp. 1615–1650.
- [6] M. BACCOUCH, *The discontinuous Galerkin method for general nonlinear third-order ordinary differential equations*, Appl. Numer. Math., 162 (2021), pp. 331–350.
- [7] M. BACCOUCH, *Superconvergence of an ultra-weak discontinuous Galerkin method for nonlinear second-order initial-value problems*, International Journal of Computational Methods, 20(2) (2023), p. 2250042.
- [8] A. BAEZA, S. BOSCARINO, P. MULET, G. RUSSO, AND D. ZORIO, *Approximate Taylor methods for ODEs*, Computers and Fluids, 159 (2017), pp. 156–166.
- [9] C. BASSI, S. BUSTO, AND M. DUMBSER, *High order ADER-DG schemes for the simulation of linear seismic waves induced by nonlinear dispersive free-surface water waves*, Appl. Numer. Math., 158 (2020), p. 236.
- [10] J. BUTCHER, *Numerical Methods for Ordinary Differential Equations*, Wiley, UK, 2016.
- [11] B. COCKBURN, S. HOU, , AND C.-W. SHU, *TVB Runge-Kutta local projection discontinuous Galerkin finite element method for conservation laws. IV. The multidimensional case*, Math. Comp., 54 (1990), pp. 545–581.
- [12] B. COCKBURN, S.-Y. LIN, AND C.-W. SHU, *TVB Runge-Kutta local projection discontinuous Galerkin finite element method for conservation laws III: One-dimensional systems*, J. Comput. Phys., 84 (1989), pp. 90–113.
- [13] B. COCKBURN AND C.-W. SHU, *TVB Runge-Kutta local projection discontinuous Galerkin finite element method for conservation laws. II. General framework*, Math. Comp., 52 (1989), pp. 411–435.
- [14] B. COCKBURN AND C.-W. SHU, *The Runge-Kutta local projection P^1 -discontinuous-Galerkin finite element method for scalar conservation laws*, ESAIM: M2AN, 25 (1991), pp. 337–361.
- [15] B. COCKBURN AND C.-W. SHU, *TVB Runge-Kutta local projection discontinuous Galerkin Method for Conservation Laws V: Multidimensional Systems*, J. Comput. Phys., 141 (1998), pp. 199–224.
- [16] K. DEKKER AND J. VERWER, *Stability of Runge-Kutta Methods for Stiff Nonlinear Differential Equations*, North-Holland, Amsterdam, 1984.
- [17] M. DELFOUR AND F. DUBEAU, *Discontinuous polynomial approximations in the theory of one-step, hybrid and multistep methods for nonlinear ordinary differential equations*, Math. Comp., 47 (1986), p. 169.
- [18] M. DELFOUR, W. HAGER, AND F. TROCHU, *Discontinuous Galerkin methods for ordinary differential equations*, Math. Comp., 36 (1981), pp. 455–473.
- [19] M. DUMBSER, *Arbitrary high order $P_N P_M$ schemes on unstructured meshes for the compressible Navier-Stokes equations*, Computers & Fluids, 39 (2010), pp. 60–76.
- [20] M. DUMBSER, C. ENAUX, AND E. TORO, *Finite volume schemes of very high order of accuracy for stiff hyperbolic balance laws*, J. Comput. Phys., 227 (2008), p. 3971.
- [21] M. DUMBSER AND O. ZANOTTI, *Very high order $P_N P_M$ schemes on unstructured meshes for the resistive relativistic mhd equations*, J. Comput. Phys., 228 (2009), p. 6991.
- [22] M. DUMBSER, O. ZANOTTI, E. GABURRO, AND I. PESHKOV, *A well-balanced discontinuous Galerkin method for the first-order Z_4 formulation of the Einstein-Euler system*, J. Comp. Phys., 504 (2024), p. 112875.
- [23] E. FERNANDEZ, M. DIAZ, M. DUMBSER, AND T. DE LUNA, *An arbitrary high order well-balanced ADER-DG numerical scheme for the multilayer shallow-water model with variable density*, J. Sci. Comput., 90 (2022), p. 52.
- [24] E. GABURRO AND M. DUMBSER, *A posteriori subcell finite volume limiter for general $P_N P_M$ schemes: Applications from gasdynamics to relativistic magnetohydrodynamics*, J. Sci. Comput., 86 (2021), p. 37.
- [25] E. GABURRO, P. OFFNER, M. RICCHIUTO, AND D. TORLO, *High order entropy preserving ADER-DG schemes*, Applied Mathematics and Computation, 440 (2023), p. 127644.
- [26] E. HAIRER, S. NØRSETT, AND G. WANNER, *Solving Ordinary Differential Equations I: Nonstiff Problems*, Springer-Verlag, Berlin, Heidelberg, 1987.
- [27] E. HAIRER AND G. WANNER, *Solving Ordinary Differential Equations II: Stiff and Differential-Algebraic Problems*, Springer-Verlag, Berlin, Heidelberg, 1996.
- [28] M. HAN VEIGA, P. OFFNER, AND D. TORLO, *DeC and ADER: Similarities, differences and a unified framework*, Journal of Scientific Computing, 87 (2021), p. 2.
- [29] A. HIDALGO AND M. DUMBSER, *ADER schemes for nonlinear systems of stiff advection-diffusion-reaction equations*, J. Sci. Comput., 48 (2011), p. 173.
- [30] A. JORBA AND M. ZOU, *A software package for the numerical integration of ODEs by means of high-order Taylor methods*, Experiment. Math., 14 (2005), pp. 99–117.

- [31] S.-C. KLEIN, *Stabilizing discontinuous Galerkin methods using Dafermos' entropy rate criterion: I — one-dimensional conservation laws*, J. Sci. Comput., 95 (2023), p. 55.
- [32] L. MICALIZZI, D. TORLO, AND W. BOSCHERI, *Efficient iterative arbitrary high-order methods: an adaptive bridge between low and high order*, Commun. Appl. Math. Comput., 7 (2023), p. 40.
- [33] I. POPOV, *Space-time adaptive ADER-DG finite element method with LST-DG predictor and a posteriori sub-cell WENO finite-volume limiting for simulation of non-stationary compressible multicomponent reactive flows*, J. Sci. Comput., 95 (2023), p. 44.
- [34] I. POPOV, *Arbitrary high order ADER-DG method with local DG predictor for solutions of initial value problems for systems of first-order ordinary differential equations*, J. Sci. Comput., 100 (2024), p. 22.
- [35] I. POPOV, *Space-time adaptive ADER-DG finite element method with LST-DG predictor and a posteriori sub-cell ADER-WENO finite-volume limiting for multidimensional detonation waves simulation*, Computers & Fluids, 284 (2024), p. 106425.
- [36] I. POPOV, *High order ADER-DG method with local DG predictor for solutions of differential-algebraic systems of equations*, J. Sci. Comput., 102 (2025), p. 48.
- [37] W. REED AND T. HILL, *Triangular mesh methods for the neutron transport equation*, Tech. Report LA-UR-73-479, Los Alamos Scientific Laboratory, 1973.
- [38] V. TITAREV AND E. TORO, *ADER: arbitrary high order Godunov approach*, J. Sci. Comput., 17 (2002), p. 609.
- [39] V. TITAREV AND E. TORO, *ADER schemes for three-dimensional nonlinear hyperbolic systems*, J. Comput. Phys., 204 (2005), p. 715.
- [40] E. TORO, V. TITAREV, M. DUMBSER, A. ISKE, C. GOETZ, C. CASTRO, G. MONTECINOS, AND D. R., *The ADER approach for approximating hyperbolic equations to very high accuracy*, in Hyperbolic Problems: Theory, Numerics, Applications. Volume I. HYP 2022. SEMA SIMAI Springer Series, vol 34., C. Pares, M. Castro, T. de Luna, and M. Muñoz-Ruiz, eds., Springer, Cham, 2024.
- [41] L. WAHLBIN, *Superconvergence in Galerkin Finite Element Methods*, Springer-Verlag, Berlin Heidelberg, 1995.
- [42] S. WOLF, M. GALIS, C. UPHOFF, A.-A. GABRIEL, M. P., D. GREGOR, AND M. BADER, *An efficient ADER-DG local time stepping scheme for 3D HPC simulation of seismic waves in poroelastic media*, J. Comp. Phys., 455 (2022), p. 110886.
- [43] O. ZANOTTI, F. FAMBRI, M. DUMBSER, AND A. HIDALGO, *Space-time adaptive ADER discontinuous Galerkin finite element schemes with a posteriori sub-cell finite volume limiting*, Computers & Fluids, 118 (2015), p. 204.